Sains Malaysiana 52(9)(2023): 2713-2723
http://doi.org/10.17576/jsm-2023-5209-19

Photoreforming of Glycerol Catalyzed by CuO/TiO_2 Supported on Hydroxyapatite

(Pemfoto Pembentukan Semula Gliserol Pemangkin oleh Cuo/Tio_2 Disokong pada Hidroksiapatit**)**

DAMRONG ADAM[1], NETNAPID ONGSUWAN[2], & SAOWAPA CHOTISUWAN[1,*]

[1]*Department of Science, Faculty of Science and Technology, Prince of Songkla University, Rusamilae, Pattani, Thailand*
[2]*Department of Food Science and Nutrition, Department of Science, Faculty of Science and Technology, Prince of Songkla University, Rusamilae, Pattani, Thailand*

Received: 23 March 2023/Accepted: 15 August 2023

ABSTRACT

Waste bovine bones can be used as a source to produce hydroxyapatite (HAp), which is a good organic adsorbent and used as a support material for metal oxide photocatalysts. In this work, HAp powders were prepared from calcination of bovine bones at 900 °C for 2 h and used as supporting material for a TiO_2 photocatalyst incorporating CuO. The hexagonal HAp particles were characterized using Fourier transformed infrared spectroscopy (FTIR), X-ray diffraction (XRD), and scanning electron microscopy (SEM). The 50 wt% TiO_2 and 1 wt% CuO/TiO_2 supported on HAp photocatalysts were synthesized by the co-precipitation method and finally calcined at 450 °C for 4 h. The synthesized HAp and catalysts were characterized by FTIR, XRD, BET surface area analysis, SEM, and transmission electron microscopy (TEM). The photocatalytic performance of the synthesized catalysts was performed by photoreforming of glycerol at room temperature using 100 mL of 0.5 M glycerol solution under nitrogen atmosphere, irradiating with low-light intensity 20 W Mercury UV lamp for 7 h. The gaseous products catalyzed by the synthesized catalysts were analyzed using a gas chromatograph. The maximum hydrogen gas production from photoreforming of glycerol at this condition was obtained at 513.7 µmol g_{cat}^{-1} without carbon dioxide detection after catalyzing by CuO/TiO_2/HAp catalyst.

Keywords: Glycerol; hydroxyapatite; photoreforming; titania

ABSTRAK

Sisa tulang lembu boleh digunakan sebagai sumber untuk menghasilkan hidroksiapatit (HAp), yang merupakan penyerap organik yang baik dan digunakan sebagai bahan sokongan untuk fotokatalis oksida logam. Dalam kertas ini, serbuk HAp disediakan daripada kalsinasi tulang lembu pada suhu 900 °C selama 2 jam dan digunakan sebagai bahan sokongan untuk fotokatalis TiO_2 yang menggabungkan CuO. Zarah HAp heksagon dicirikan menggunakan spektroskopi inframerah Fourier berubah (FTIR), pembelahan sinar-X (XRD) dan mikroskop elektron imbasan (SEM). 50 wt% TiO_2 dan 1 wt% CuO/TiO_2 yang disokong pada fotokatalis HAp disintesis oleh kaedah pemendakan bersama dan akhirnya dikalsinasi pada 450 °C untuk 4 jam. HAp dan pemangkin yang disintesis dicirikan oleh FTIR, XRD, ANALISIS kawasan permukaan BET, SEM dan mikroskop elektron penghantaran (TEM). Prestasi fotokatalisis pemangkin yang disintesis dilakukan dengan pembentukan semula foto gliserol pada suhu bilik menggunakan 100 mL 0.5 M. Penyelesaian gliserol di bawah atmosfera nitrogen, mengairi dengan keamatan cahaya rendah 20 W Mercury UV lampu untuk 7 jam. Produk gas yang pemangkin oleh pemangkin yang disintesis telah dianalisis menggunakan kromatograf gas. Pengeluaran gas hidrogen maksimum daripada pembentukan semula gliserol dalam keadaan ini diperoleh pada 513.7 µmol $gcat^{-1}$ tanpa pengesanan karbon dioksida selepas pemangkin oleh pemangkin CuO/TiO_2/HAp.

Kata kunci: Gliserol; hidroksiapatit; pemfoto pembentukan semula; titania

INTRODUCTION

Byproducts from biodiesel production such as glycerol can be used as raw materials for many chemicals, e.g., 1, 2-propanediol (Azri et al. 2022; Liu et al. 2021), acrolein (Galadima & Muraza 2016), lactic acid (Arcanjo et al. 2017, Yin et al. 2016), and hydrogen gas (Estahbanati et al. 2021; Liu et al. 2014; Lucchetti et al. 2017; Yang et al. 2020). Hydrogen gas can be obtained from photoreforming

of glycerol by catalyzing it with photocatalysts such as titania (TiO_2) (Kozlova et al. 2020) and zinc oxide (ZnO) (Montini et al. 2016). The overall reaction catalyzed by a photocatalyst and irradiated with UV or visible light is shown in equation (1).

$$C_3H_8O_3\ (l) + 3H_2O\ (l) \rightarrow 3CO_2\ (g) + 7H_2\ (g) \qquad (1)$$

Most photoreforming of glycerol reactions catalyzed by photocatalysts incorporate doping metals but not support materials (Sang et al. 2012; Wang et al. 2017; Seadira et al. 2017; Yang et al. 2020). Titania is the most widely used photocatalyst because of its stability, availability, and resistance to photo-corrosion, but the fast recombination of electron–hole pairs, spontaneous aggregation of TiO_2 particles in the aqueous phase, and high bandgap value (3.2 eV) have to be improved (Escamilla et al. 2020; Yang et al. 2020). The photocatalyst or active phase can be dispersed on supporting materials, enhancing the surface area of active catalysts and reducing catalyst aggregation during the reaction. Supporting materials for titania photocatalysts have been studied, e.g., mesoporous carbon (Escamilla et al. 2020), metal organic frameworks (MOFs) (Martínez et al. 2019), and hydroxyapatite (Nguyen Thi Truc, Hong & No 2019). Due to their physicochemical properties, such as good organic adsorption property (El Bekkali et al. 2018), and optical properties with bandgap energy around 5-6 eV, hydroxyapatite or HAp ($Ca_{10}(PO_4)_6(OH)_2$) can be used as a support for photocatalysts that catalyze the decomposition of organic contaminants such as acetone and organic dyes (Nguyen Thi Truc, Hong & No 2019).

HAp can be synthesized using calcium ions and phosphoric acid as precursors and with natural precursors such as animal bones, e.g., bovine (Akram et al. 2014; Barakat et al. 2009; Hernández-Barreto, Hernández-Cocoletzi & Moreno-Piraján 2022), mutton (Singh, Chakraborty & Gupta 2018), pig (Ramirez-Gutierrez et al. 2017), chicken, salmon (Van Nguyen et al. 2022), or fish scales (Foroutan et al. 2021; Safronova et al. 2022), and eggshells (Das Lala et al. 2021).

In this article, waste bovine bones from a local restaurant in Pattani province, Thailand, were used as a precursor to synthesized HAp and as a support for titania photocatalyst incorporating some metal oxides such as copper(II) oxide to increase its activity. The photoreforming of glycerol to produce hydrogen gas was performed at room temperature under UV irradiation.

EXPERIMENTAL PROCEDURE

MATERIALS

All chemicals, e.g., potassium hydroxide (Loba Chemie, India), sodium hydroxide (Loba Chemie, India), titanium dioxide powder (Riedel-de Haën, Germany), copper(II) nitrate hemipentahydrate [$Cu(NO_3)_2.2.5H_2O$] (Ajax Finechem, Australia), nickel(II) nitrate hexahydrate [$Ni(NO_3)_2.6H_2O$] (Ajax Finechem, Australia), and silver nitrate ($AgNO_3$) (Merck, Germany) were analytical grade (> 99 % purity) and were used as received without purification.

SYNTHESIS OF HAP FROM BOVINE BONES

Waste bovine bones were collected from a meat soup restaurant located in Mueang district, Pattani province, rinsed with deionized water, soaked with a 5 wt% sodium hydroxide solution, and then heated to 121 °C in an autoclave at a pressure 15 $lb_f\ in^{-2}$ for 2 h to remove protein and collagen. Cleaned bovine bones were dried in a hot air oven at 105 °C, cut into small pieces, and calcined at 900 °C for 2 h to obtain pale yellow HAp. The synthesized HAp was ground into a fine powder and separated through a sieve of 325 mesh to be uses as catalyst support.

PREPARATION OF 50 WT % TIO_2 SUPPORTED ON HAP

The TiO_2 supported on HAp (50-50 wt%) photocatalysts was prepared by the co-precipitation method. Firstly, 2 g TiO_2 and 2 g HAp (325 mesh) were dispersed in deionized water, vigorously stirred, and then sonicated for 15 min. The 10 mL of 2.0 M KOH solution was added dropwise until pH 12-13 under stirring, then continuously stirred for 20 h. The mixture was centrifuged at 3000 rpm for 15 min to separate the white solids of TiO_2/HAp. The product was washed with deionized water several times, dried at 80 °C for 6 h, and calcined at 450 °C for 3 h.

PREPARATION OF 1 WT % M/TIO_2 SUPPORTED ON HAP

The 1 wt% M/TiO_2 supported on the HAp catalyst was prepared by the co-precipitation method (M was CuO, NiO, and Ag_2O). Briefly, TiO_2 powder was stirred in $Cu(NO_3)_2.2.5H_2O$ solution for 10 min, then HAp (325 mesh) was slowly added. The mixture was sonicated for 15 min, then slowly added dropwise 2.0 M KOH until pH 12–13 under stirring. The mixture was continuously stirred for 20 h, centrifuged to separate white solids, washed with deionized water several times, and dried at 80 °C for 6 h. Finally, it was calcined at 450 °C for 3 h to obtain 1 wt% CuO/TiO_2 supported on HAp. NiO/TiO_2/

HAp and Ag_2O/TiO_2/HAp were also prepared using the same method as CuO/TiO_2/HAp but using $Ni(NO_3)_2.6H_2O$ and $AgNO_3$ precursors.

CHARACTERIZATION OF HAP, TIO_2, AND M/TIO_2 SUPPORTED ON HAP

The synthesized HAp, TiO_2 supported on HAp, and M/TiO_2 supported on HAp catalysts were characterized using various techniques. The phase and crystallinity of HAp and photocatalysts were analyzed by X-ray diffractometer (XRD) (Philips, X'Pert MPD, Netherlands) using Cu K_α as X-ray source (λ = 0.154 nm) generated with 40 kV, 30 mA, scan step size (2θ) 0.05° min^{-1} in the 2θ range 10–80°. The morphology was characterized by scanning electron microscope (SEM) (FEI, Quanta 400, Czech Republic), and the surface functional groups were analyzed by Fourier transform infrared spectrophotometer (FTIR) (Bruker, Tensor 27, Germany) with 32 scans with a resolution of 4 cm^{-1} in the range 400–4000 cm^{-1}. The BET surface area of TiO_2/HAp and CuO/TiO_2/HAp samples was analyzed by a BET surface area analyzer (Micromeritics, ASAP 2460, USA). The bandgap energy of catalysts was also characterized by a diffuse reflectance UV–visible spectrophotometer (Shimadzu, UV–2600) in the range 400-4000 nm.

PHOTOREFORMING OF GLYCEROL CATALYZED BY TIO_2 AND M/TIO_2 SUPPORTED ON HAP

After purging the system with N_2 gas for 1 h, 0.2 wt% photocatalysts were added to a 250 mL two-neck round bottom flask containing 100 mL of 0.5 M glycerol solution under stirring and kept in the dark for 1 h to reach the adsorption-desorption equilibrium of the methylene blue solution on the catalyst. The photoreforming of glycerol reaction started when the irradiation reactor was irradiated with a 20 W mercury UV lamp at room temperature for 7 h, with a low light intensity of 0.042 W m^{-2}. The 0.5 mL of gaseous products were collected and analyzed by a gas chromatograph equipped with a thermal conductivity detector (GC–TCD) (Shimadzu, 14A) using Ar gas as the carrier gas.

STATISTICAL ANALYSIS

Each experiment in this work was performed at least three times and analyzed by the basic statistical method using mean and standard deviation values to ensure the reliability, precision, and trends of the data.

RESULTS AND DISCUSSION

THE CHEMICAL PROPERTY OF HAP, TiO_2, AND CuO/TiO_2 SUPPORTED ON HAP

Pale yellow HAp powders were obtained from bovine bones after NaOH solution pretreatment and calcination at 900 °C for 2 h. The chemical composition of synthesized HAp is shown in Table 1.

There were some impurities such as carbon in the form of carbonates (showing a FTIR peak in Figure 1), sodium, and magnesium. The molar ratio between Ca and P in this work was 1.61, which is nearly the same as pure hydroxyapatite (1.67). Normally, commercial HAp has a Ca:P molar ratio of about 1.57-1.70 (Bano et al. 2017; LeGeros 1988). The functional groups of the synthesized HAp from bovine bones were characterized by KBr pellets–FTIR, as shown in Figure 1.

The organic functional groups not found in Figure 1 indicate that they were completely burned out at 900 °C for 2 h. The bending of the –OH group was found at 632.6 cm^{-1} (OH bending), 3572.0 cm^{-1} (OH stretching). The broad peak at 3,300–3,600 cm^{-1} presented the hydrogen bond of hydroxyl groups. The FTIR peaks occurred at 569.0 and 601.8 cm^{-1} indicating phosphate bending, while peaks at 960.5, 1049.2, and 1089.7 cm^{-1} represent the stretching of PO_4^{3-} groups. The FTIR peaks at 1458.1 and 1415.7 cm^{-1} indicated a carbonate (CO_3^{2-}) group on HAp surface, which can adsorb carbon dioxide gas (Cheng et al. 1988; Khoo et al. 2015*)*. As a result of adding TiO_2 to the surface of the HAp with a ratio of 50:50 wt%, it was found that the maximum absorption range peaked at the wavelength range 400-800 cm^{-1}. This peak shows the characteristic vibration of Ti-O bonding at wavenumbers 653.84 and 497.61 cm^{-1}. The interaction between Ti-O bonding of the TiO_2 catalyst connected to -OH groups at the surface of the HAp (Figure 1) (Chong et al. 2018) was observed by decreasing the intensity of the hydroxyl peak for the TiO2/HAp catalyst compared to bare HAp.

TABLE 1. Chemical composition of HAp synthesized from bovine bones

Elements	Ca	P	Na	C	O	Mg
Composition (wt % ± SD)	34.65 ± 0.67	16.68 ± 0.18	1.53 ± 0.08	4.98 ± 0.39	41.55 ± 0.60	0.61 ± 0.03

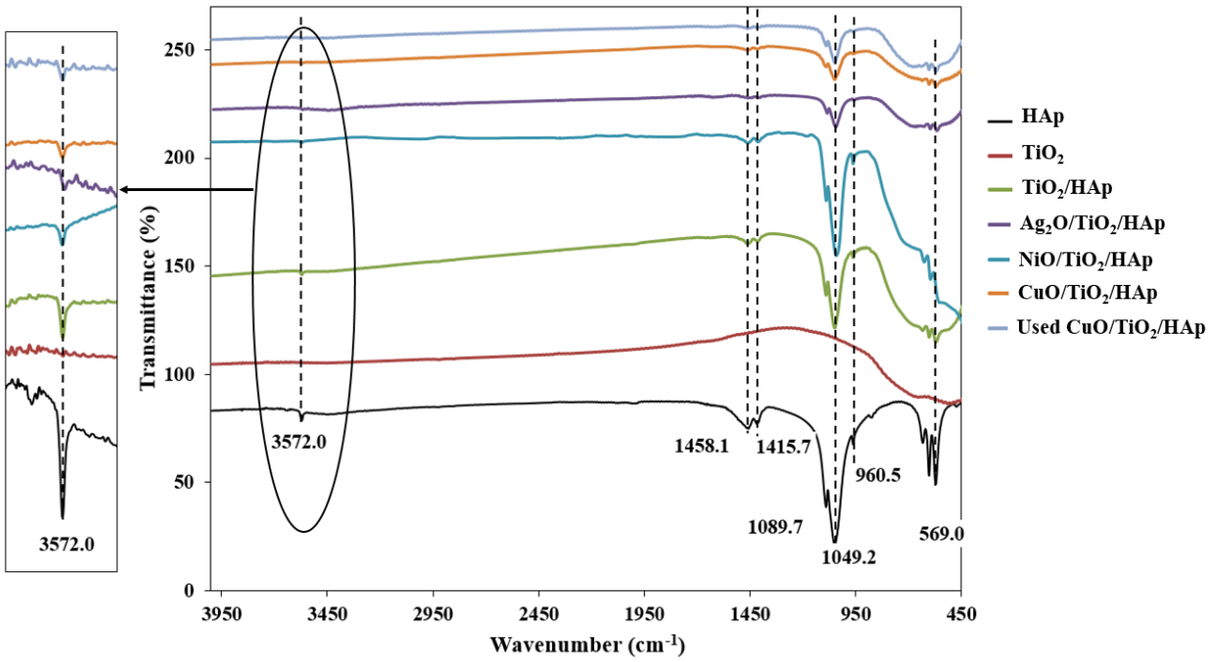

FIGURE 1. FTIR spectra of HAp synthesized from bovine bones, TiO_2, TiO_2/HAp, CuO/TiO_2/HAp, Ag_2O/TiO_2/HAp, NiO/TiO_2/HAp, and used CuO/TiO_2/HAp

The XRD pattern of HAp powder synthesized from bovine bone presented in Figure 2 represents the main diffraction angle 2θ at 31.83°, 32.23°, and 32.98° for crystal plans (211), (112), and (300), respectively. Other diffraction angles were found at 25.93° (002), 34.13° (202), 39.88° (310), 46.78° (222), and 49.53° (213). This XRD pattern indicated characteristics of HAp according to JCPDS–ICDD No. 09–0432, showing hexagonal crystals with a P63/m space group *(*Khoo et al. 2015*)*. The XRD pattern of titania was found at 2θ angles of 25.8° (101), 37.7° (004), 48.0° (200), 53.8° (105), and 55.0° (211), showing pure anatase phase according to JCPDS No. 21–1272 (Peter Etape et al. 2017). The diffraction angles of TiO_2 supported on HAp and CuO/TiO_2/HAp in Figure 2 did not change compared to bare titania and HAp representing good titania in the form of anatase dispersion on HAp. However, the diffraction angle at 2θ about 35.7° indicating CuO (Liu et al. 2014) was not observed, possibly due to the small amount of CuO and good dispersion of CuO particles. The crystal sizes of TiO_2, TiO_2/HAp, and M/TiO_2/HAp calculated by the Scherer equation (Peter Etape et al. 2017*)* using 2θ diffraction angles at 25.3° were around 48.4-49.1 nm, larger than the TiO_2 particle sizes prepared by other research work (Hu et al. 2018; Peter Etape et al. 2017; Singh, Chakraborty & Gupta 2018).

MORPHOLOGY OF HAP, TIO_2, AND CuO/TiO_2 SUPPORTED ON HAp

The particles of synthesized HAp were characterized by SEM, as shown in Figure 3. Figure 3(a) denotes a cluster of HAp hexagonal crystal shapes with 800-1200 nm in diameters, and Figure 3(b) represents the morphology of synthesized TiO_2 with a spherical shape and particle size dispersion around 90-250 nm. Some TiO_2 particles can be adsorbed on HAp surface after synthesizing TiO_2/HAp by co-precipitation (Figure 3(c)). However, aggregation of TiO_2 particles was also observed. The morphology of TiO_2 and HAp particles did not change after adding CuO, Ag_2O, and NiO particles to form CuO/TiO_2/HAp, Ag_2O/TiO_2/HAp, and NiO/TiO_2/HAp, respectively, as shown in Figure 3(d)-3(f). The SEM images could not clearly show CuO, Ag_2O, and NiO particles due to metal oxide's small amount and nanometer size on TiO_2. Additionally, SEM-EDX shows the amount of metal oxides on these catalysts was 1 wt%, and the BET surface area of the TiO_2/HAp catalyst was 14.01 m^2 g^{-1} and decreased to

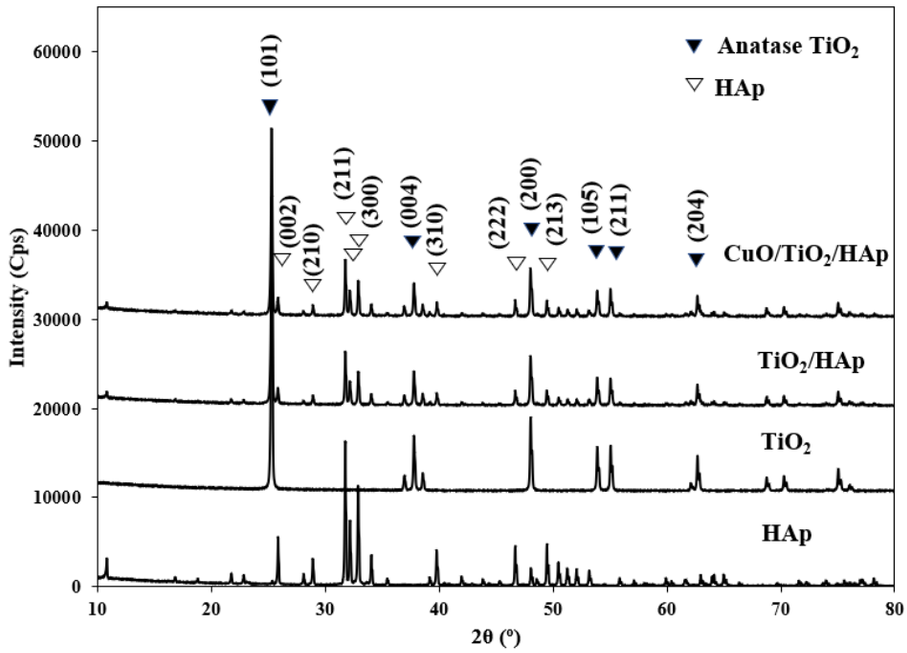

FIGURE 2. XRD patterns of HAp synthesized from bovine bones, TiO_2, TiO_2/HAp, and CuO/TiO_2/HAp

6.34 m^2 g^{-1} for the CuO/TiO_2/HAp sample due to the adsorption of CuO particles on the catalyst surface.

The morphology of TiO_2/HAp and CuO/TiO_2/HAp catalysts was further characterized by TEM as shown in Figures 4(a) and 4(b), indicating TiO_2 particles with 50–200 nm in diameter dispersed on HAp particles (600–800 nm), whereas nanometer-size of CuO particles (5–20 nm) adsorbed on TiO_2 surfaces. However, the particle size of CuO did not uniformly disperse on TiO_2 surfaces compared to CuO_x/TiO_2 synthesized by Kozlova et al. (2020) using $NaBH_4$ as a reducing agent.

BANDGAP ENERGY

Synthesized HAp, TiO_2, and M/TiO_2/HAp catalysts were characterized by DRS UV–Vis spectroscopy, and bandgap energy was calculated as shown in Table 2.

The HAp can absorb light with a wavelength less than 200 nm, and the bandgap energy is 7.16 eV. The bandgap energy of synthesized TiO_2 was 3.46 eV, larger than pure anatase TiO_2 (3.2 eV). However, it remains in the range of 3.2-3.6 eV for TiO_2 (Haider, Jameel & Al-Hussaini 2019). The addition of 50 wt% TiO_2 to HAp did not significantly change the bandgap energy (3.46 eV) of TiO_2, indicating that the crystal structure of TiO_2 and HAp did not change; this bandgap energy was nearly the same as TiO_2/HAp synthesized by other groups (Hu et al. 2018). The bandgap energy of CuO/TiO_2/HAp, NiO/TiO_2/HAp, and Ag_2O/TiO_2/HAp was 3.50, 3.48, and 3.52 eV, respectively, which is slightly higher than bare TiO_2. This is possibly due to fewer metal oxides and poor dispersion on the TiO_2 surface. From these results, synthesized photocatalysts can absorb UV light at a wavelength of 350-356 nm.

CATALYTIC PERFORMANCE OF PHOTOREFORMING OF GLYCEROL BY CUO/TIO$_2$ SUPPORTED ON HAp

The photoreforming of glycerol was catalyzed by TiO_2 and M/TiO_2/HAp using 0.20 wt% catalyst, 100 mL of 0.5 mol L^{-1} glycerol solution at 35 °C, and irradiated with a low-light intensity 20 W mercury UV lamp under an N_2 atmosphere. The hydrogen production (μmol g_{cat}^{-1}) during the 7 h reaction time is shown in Figure 5.

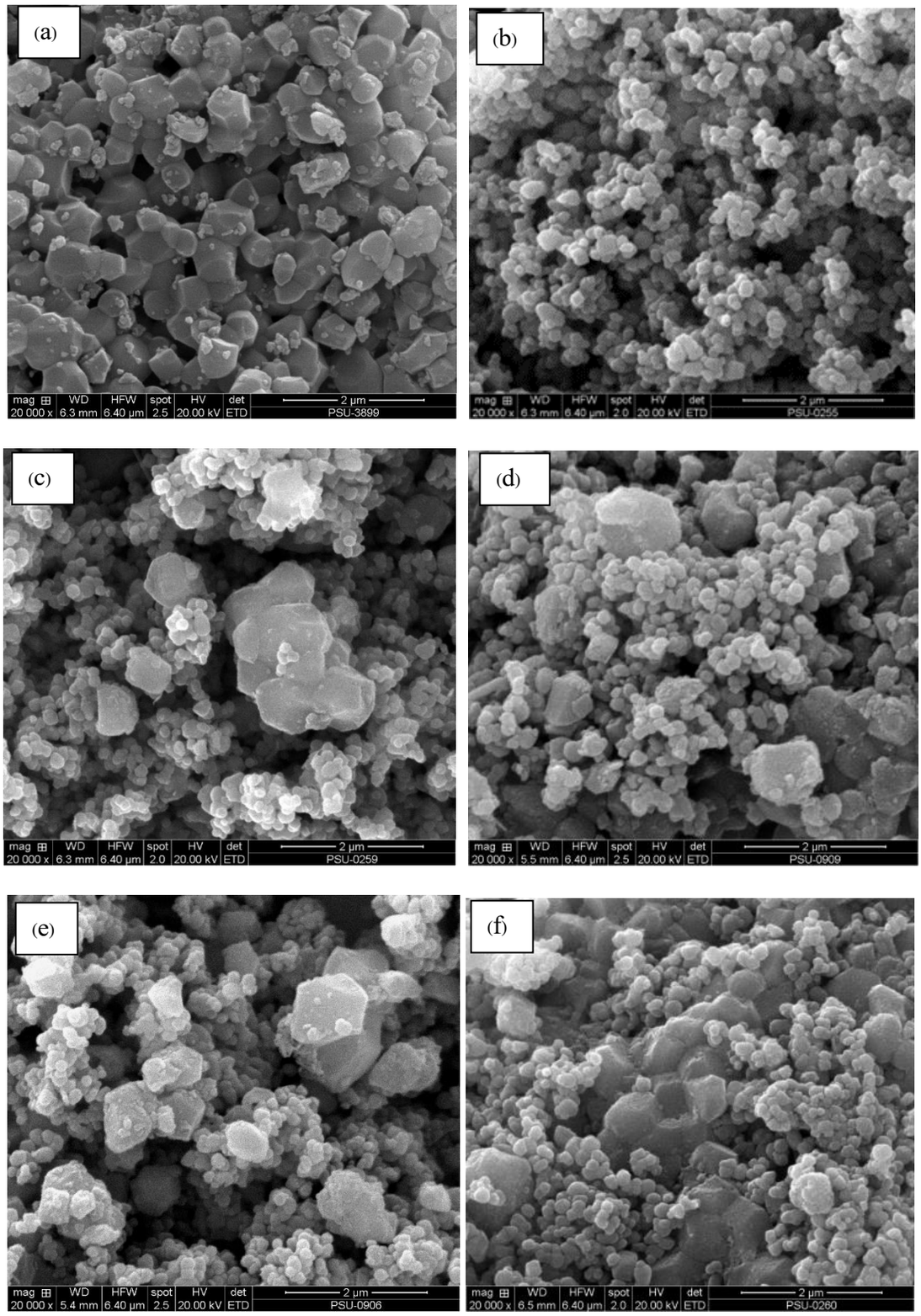

FIGURE 3. SEM images of (a) HAp synthesized from bovine bone, (b) TiO_2, (c) TiO_2/HAp, (d) CuO/TiO_2/HAp, (e) Ag_2O/TiO_2/HAp, and (f) NiO/TiO_2/HAp (20,000x)

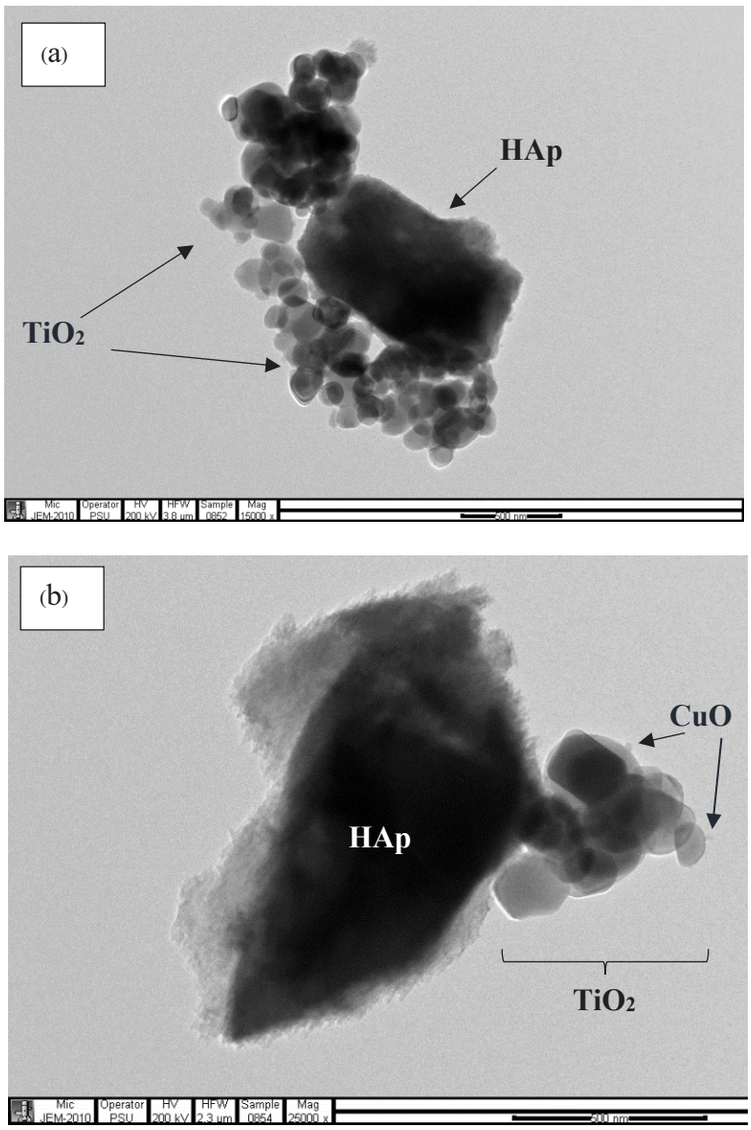

FIGURE 4. TEM images of (a) TiO_2/HAp (15,000x), and (b) CuO/TiO_2/HAp represent the dispersion of CuO particles on TiO_2/HAp (25,000x)

TABLE 2. Band gap energy of M/TiO_2/HAp calculated from DRS UV–Vis spectroscopy data

Samples	Bandgap energy, E_g (eV)	λ_{max} (nm)
HAp	7.16	173
TiO_2	3.46	358
TiO_2/HAp	3.46	358
CuO/TiO_2/HAp	3.50	356
NiO/TiO_2/HAp	3.48	354
Ag_2O/TiO_2/HAp	3.52	350

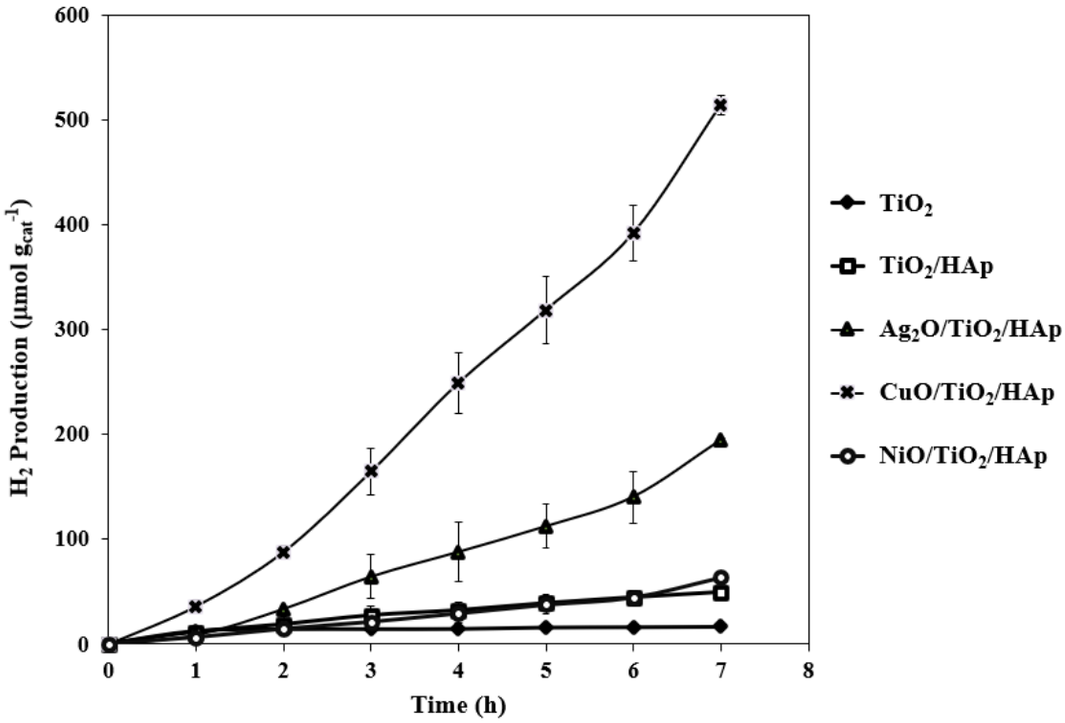

FIGURE 5. Hydrogen production from photoreforming of glycerol catalyzed by TiO_2 and M/TiO_2/HAp; 0.20 wt % catalyst, 100 mL 0.5 mol L^{-1} glycerol solution, 7 h reaction time, irradiated with a low-light intensity 20 W mercury UV lamp, N_2 atmosphere, 35 °C

The gas product from the reaction was detected using GC–TCD. Only hydrogen gas was found, and no sign of carbon dioxide gas was observed. From Figure 5, the maximum catalytic performance for photoreforming of glycerol was as follows: CuO/TiO_2/HAp >> Ag_2O/TiO_2/HAp >> NiO/TiO_2/HAp >> TiO_2/HAp >> TiO_2 shows hydrogen production at 513.66, 194.25, 63.70, 49.62, and 16.61 µmol g_{cat}^{-1}, respectively, at 7 h. The TiO_2/HAp showed higher hydrogen gas production than bare TiO_2 due to the good dispersion of TiO_2 on HAp confirmed by SEM and TEM, and good chemisorption of organic molecules on HAp, which resulted in the photocatalytic performance of TiO_2/HAp (Hu et al. 2018). Additionally, the electronic state of phosphate groups on the HAp surface can change and generate active superoxide anion radicals during UV radiation of the photocatalyst (Nguyen Thi Truc, Hong & No 2019). The active superoxide anion radicals can further react with adsorbed organic molecules. The TiO_2/HAp catalyst incorporating metal oxides, especially CuO, can reduce electron-hole recombination during photocatalysis (Kozlova et al. 2020; Liu et al. 2014; Seadira et al. 2018; Wang et al. 2017), as shown in Figure 6.

Furthermore, in this work, no carbon dioxide gas product from the reaction was detected by GC-TCD. It might be possible that carbon dioxide gas produced from the reaction was adsorbed on the HAp surface through hydroxyl and phosphate groups (Nguyen Thi Truc, Hong & No 2019; Mohseni-Salehi, Taheri-Nassaj & Hosseini-Zori 2018). The adsorption of carbonate can interact with the hydroxyl and phosphate groups of HAp (Chong et al. 2018). The CuO/TiO_2/HAp catalysts were also tested for catalytic regeneration by simply soaking the used catalysts in ethanol for 12 h and drying at 60 °C for 1 h without calcination. It was observed that the catalytic performances of photoreforming of glycerol for three catalytic cycles were significantly decreased by *ca.* 18%, possibly due to the reduction of Cu(II) to Cu(I) and the aggregation of copper metal particles (Kozlova et al. 2020).

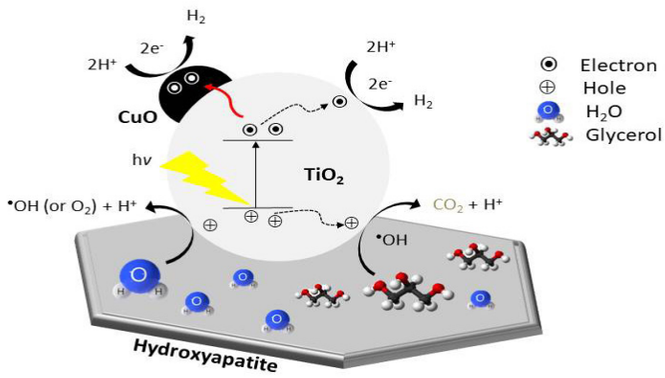

FIGURE 6. The possible photocatalytic mechanism for the catalytic performance of photoreforming of glycerol by CuO/TiO_2 supported on HAp

CONCLUSIONS

The HAp powders with a 1.61 Ca/P molar ratio were successfully prepared from waste bovine bones after calcination at 900 °C for 2 h and used as good supporting material for photocatalysts. The CuO/TiO_2/HAp, Ag_2O/TiO_2/HAp, and NiO/TiO_2/HAp catalysts prepared by co-precipitation were active for photoreforming of glycerol irradiated with a low-light intensity 20 W UV lamp under N_2 atmosphere at 35 °C with hydrogen production at 513.66, 194.25, and 63.70 µmol g_{cat}^{-1}, respectively, at 7 h without detection of CO_2 gas product.

ACKNOWLEDGEMENTS

This work was financially supported by the Research Fund of Prince of Songkla University, Pattani campus (SAT600800S), Thailand.

REFERENCES

Akram, M., Ahmed, R., Shakir, I., Ibrahim, W.A.W. & Hussain, R. 2014. Extracting hydroxyapatite and its precursors from natural resources. *Journal of Materials Science* 49(4): 1461-1475. https://doi.org/10.1007/s10853-013-7864-x

Arcanjo, M.R.A., Silva, I.J., Rodríguez-Castellón, E., Infantes-Molina, A. & Vieira, R.S. 2017. Conversion of glycerol into lactic acid using Pd or Pt supported on carbon as catalyst. *Catalysis Today* 279: 317-326. https://doi.org/10.1016/j.cattod.2016.02.015

Azri, N., Irmawati, R., Yda-Umar, U.I., Saiman, M.I. & Taufiq-Yap, Y.H. 2022. Effect of different metal modified dolomite catalysts on catalytic glycerol hydrogenolysis towards 1,2-propanediol. *Sains Malaysiana* 51(5): 1385-1398. https://doi.org/10.17576/jsm-2022-5105-10

Bano, N., Salwah Jikan, S., Basri, H., Adzila Abu Bakar, S.S. & Hussain Nuhu, A. 2017. Natural hydroxyapatite extracted from bovine bone. *Journal of Science and Technology* 9(2): 22-28. https://publisher.uthm.edu.my/ojs/index.php/JST/article/view/1990

Barakat, N.A.M., Khil, M.S., Omran, A.M., Sheikh, F.A. & Kim, H.Y. 2009. Extraction of pure natural hydroxyapatite from the bovine bones bio waste by three different methods. *Journal of Materials Processing Technology* 209(7): 3408-3415. https://doi.org/10.1016/j.jmatprotec.2008.07.040

Cheng, Z.H., Yasukawa, A., Kandori, K. & Ishikawa, T. 1998. FTIR study of adsorption of CO_2 on nonstoichiometric calcium hydroxyapatite. *Langmuir* 14(23): 6681-6686. https://doi.org/10.1021/la980339n

Chong, R., Fan, Y., Du, Y., Liu, L., Chang, Z. & Li, D. 2018. Hydroxyapatite decorated TiO_2 as efficient photocatalyst for selective reduction of CO_2 with H_2O into CH_4. *International Journal of Hydrogen Energy* 43(49): 22329-22339. https://doi.org/10.1016/j.ijhydene.2018.10.045

Das Lala, S., Barua, E., Deb, P. & Deoghare, A.B. 2021. Physico-chemical and biological behaviour of eggshell bio-waste derived nano-hydroxyapatite matured at different aging time. *Materials Today Communications* 27: 102443. https://doi.org/10.1016/j.mtcomm.2021.102443

El Bekkali, C., Bouyarmane, H., El Karbane, M., Masse, S., Saoiabi, A., Coradin, T. & Laghzizil, A. 2018. Zinc oxide-hydroxyapatite nanocomposite photocatalysts for the degradation of ciprofloxacin and ofloxacin antibiotics. *Colloids and Surfaces A: Physicochemical and Engineering Aspects* 539: 364-370. https://doi.org/10.1016/j.colsurfa.2017.12.051

Escamilla, J.C., Hidalgo-Carrillo, J., Martín-Gómez, J., Estévez-Toledano, R.C., Montes, V., Cosano, D., Urbano, F.J. & Marinas, A. 2020. Hydrogen production through glycerol photoreforming on TiO_2/mesoporous carbon: Influence of the synthetic method. *Materials* 13(17): 3800. https://doi.org/10.3390/MA13173800

Foroutan, R., Peighambardoust, S.J., Hosseini, S.S., Akbari, A. & Ramavandi, B. 2021. Hydroxyapatite biomaterial production from chicken (femur and beak) and fishbone waste through a chemical less method for Cd^{2+} removal from shipbuilding wastewater. *Journal of Hazardous Materials* 413: 125428. https://doi.org/10.1016/j.jhazmat.2021.125428

Galadima, A. & Muraza, O. 2016. A review on glycerol valorization to acrolein over solid acid catalysts. *Journal of the Taiwan Institute of Chemical Engineers* 67: 29-44. https://doi.org/10.1016/j.jtice.2016.07.019

Haider, A.J., Jameel, Z.N. & Al-Hussaini, I.H.M. 2019. Review on: Titanium dioxide applications. *Energy Procedia* 157: 17-29. https://doi.org/10.1016/j.egypro.2018.11.159

Hernández-Barreto, D.F., Hernández-Cocoletzi, H. & Moreno-Piraján, J.C. 2022. Biogenic hydroxyapatite obtained from bone wastes using CO_2-assisted pyrolysis and its interaction with glyphosate: A computational and experimental study. *ACS Omega* 7(27): 23265-23275. https://doi.org/10.1021/acsomega.2c01379

Hu, M., Yao, Z., Liu, X., Ma, L., He, Z. & Wang, X. 2018. Enhancement mechanism of hydroxyapatite for photocatalytic degradation of gaseous formaldehyde over TiO_2/hydroxyapatite. *Journal of the Taiwan Institute of Chemical Engineers* 85: 91-97. https://doi.org/10.1016/j.jtice.2017.12.021

Karimi Estahbanati, M.R., Feilizadeh, M., Attar, F. & Iliuta, M.C. 2021. Current developments and future trends in photocatalytic glycerol valorization: Process analysis. *Reaction Chemistry and Engineering* 6(2): 197-219. https://doi.org/10.1039/d0re00382d

Khoo, W., Nor, F.M., Ardhyananta, H. & Kurniawan, D. 2015. Preparation of natural hydroxyapatite from bovine femur bones using calcination at various temperatures. *Procedia Manufacturing* 2: 196-201. https://doi.org/10.1016/j.promfg.2015.07.034

Kozlova, E.A., Gromov, N.V., Saraev, A.A., Kaichev, V.V., Gromov, N.V., Medvedeva, T.B., Saraev, A.A. & Kaichev, V.V. 2020. Comparative study of photoreforming of glycerol on Pt/TiO_2 and CuO_x/TiO_2. *Materials Letters* 283: 128901. https://doi.org/10.1016/j.matlet.2020.128901

LeGeros, R.Z. 1988. Calcium phosphate materials in restorative dentistry: A review. *Advances in Dental Research* 2(1): 164-180. https://doi.org/10.1177/08959374880020011101

Liu, R., Yoshida, H., Fujita, S. & Arai, M. 2014. Photocatalytic hydrogen production from glycerol and water with NiO_x/TiO_2 catalysts. *Applied Catalysis B: Environmental* 144: 41-45. https://doi.org/10.1016/j.apcatb.2013.06.024

Liu, Y., Wu, M., Rempel, G.L. & Ng, F.T.T. 2021. Glycerol hydrogenolysis to produce 1,2-propanediol in absence of molecular hydrogen using a Pd promoted Cu/MgO/Al_2O_3 catalyst. *Catalysts* 11(11): 1299. https://doi.org/10.3390/catal11111299

Lucchetti, R., Onotri, L., Clarizia, L., Di Natale, F., Di Somma, I., Andreozzi, R. & Marotta, R. 2017. Removal of nitrate and simultaneous hydrogen generation through photocatalytic reforming of glycerol over "*in situ*" prepared zero-valent nano copper/P25. *Applied Catalysis B: Environmental* 202: 539-549. https://doi.org/10.1016/j.apcatb.2016.09.043

Martínez, F.M., Albiter, E., Alfaro, S., Luna, A.L., Colbeau-Justin, C., Barrera-Andrade, J.M., Remita, H. & Valenzuela, M.A. 2019. Hydrogen production from glycerol photoreforming on TiO_2/HKUST-1 composites: Effect of preparation method. *Catalysts* 9(4): 1-12. https://doi.org/10.3390/catal9040338

Mohseni-Salehi, M.S., Taheri-Nassaj, E. & Hosseini-Zori, M. 2018. Effect of dopant (Co, Ni) concentration and hydroxyapatite compositing on photocatalytic activity of titania towards dye degradation. *Journal of Photochemistry and Photobiology A: Chemistry* 356: 57-70. https://doi.org/10.1016/j.jphotochem.2017.12.027

Montini, T., Monai, M., Beltram, A., Romero-Ocaña, I. & Fornasiero, P. 2016. H_2 production by photocatalytic reforming of oxygenated compounds using TiO_2-based materials. *Materials Science in Semiconductor Processing* 42: 122-130. https://doi.org/10.1016/j.mssp.2015.06.069

Nguyen Thi Truc, L., Hong, S. & No, K. 2019. Evaluation of the role of hydroxyapatite in TiO_2/hydroxyapatite photocatalytic materials. *Photocatalysts - Applications and Attributes.* March. *IntechOpen*. https://doi.org/10.5772/intechopen.81092

Peter Etape, E., John Ngolui, L., Foba-Tendo, J., Yufanyi, D.M. & Victorine Namondo, B. 2017. Synthesis and characterization of CuO, TiO_2, and CuO-TiO_2 mixed oxide by a modified oxalate route. *Journal of Applied Chemistry* 2017: 4518654. https://doi.org/10.1155/2017/4518654

Ramirez-Gutierrez, C.F., Londoño-Restrepo, S.M., del Real, A., Mondragón, M.A. & Rodriguez-García, M.E. 2017. Effect of the temperature and sintering time on the thermal, structural, morphological, and vibrational properties of hydroxyapatite derived from pig bone. *Ceramics International* 43(10): 7552-7559. https://doi.org/10.1016/j.ceramint.2017.03.046

Safronova, T., Vorobyov, V., Kildeeva, N., Shatalova, T., Toshev, O., Filippov, Y., Dmitrienko, A., Gavlina, O., Chernega, O., Nizhnikova, E., Akhmedov, M., Kukueva, E. & Lyssenko, K. 2022. Inorganic powders prepared from fish scales. *Ceramics* 5(3): 484-498. https://doi.org/10.3390/ceramics5030037

Sang, H.X., Wang, X.T., Fan, C.C. & Wang, F. 2012. Enhanced photocatalytic H_2 production from glycerol solution over ZnO/ZnS core/shell nanorods prepared by a low temperature route. *International Journal of Hydrogen Energy* 37(2): 1348-1355. https://doi.org/10.1016/j.ijhydene.2011.09.129

Seadira, T.W.P., Sadanandam, G., Ntho, T., Masuku, C.M. & Scurrell, M.S. 2018. Preparation and characterization of metals supported on nanostructured TiO_2 hollow spheres for production of hydrogen via photocatalytic reforming of glycerol. *Applied Catalysis B: Environmental* 222: 133-145. https://doi.org/10.1016/j.apcatb.2017.09.072

Singh, N., Chakraborty, R. & Gupta, R.K. 2018. Mutton bone derived hydroxyapatite supported TiO_2 nanoparticles for sustainable photocatalytic applications. *Journal of Environmental Chemical Engineering* 6(1): 459-467. https://doi.org/10.1016/j.jece.2017.12.027

Van Nguyen, T.T., Phung Anh, N., Ho, T.G.T., Pham, T.T.P., Nguyen, P.H.D., Do, B.L., Huynh, H.K.P. & Nguyen, T. 2022. Hydroxyapatite derived from salmon bone as green ecoefficient support for ceria-doped nickel catalyst for CO_2 methanation. *ACS Omega* 7(41): 36623-36633. https://doi.org/10.1021/acsomega.2c04621

Wang, C., Cai, X., Chen, Y., Cheng, Z., Luo, X., Mo, S., Jia, L., Lin, P. & Yang, Z. 2017. Improved hydrogen production from glycerol photoreforming over sol-gel derived TiO_2 coupled with metal oxides. *Chemical Engineering Journal* 317: 522-532. https://doi.org/10.1016/j.cej.2017.02.033

Yang, Z., Zhong, W., Chen, Y., Wang, C., Mo, S., Zhang, J., Shu, R. & Song, Q. 2020. Improving glycerol photoreforming hydrogen production over Ag_2O-TiO_2 catalysts by enhanced colloidal dispersion stability. *Frontiers in Chemistry* 8: 342. https://doi.org/10.3389/fchem.2020.00342

Yin, H., Zhang, C., Yin, H., Gao, D., Shen, L. & Wang, A. 2016. Hydrothermal conversion of glycerol to lactic acid catalyzed by Cu/hydroxyapatite, Cu/MgO, and Cu/ZrO_2 and reaction kinetics. *Chemical Engineering Journal* 288: 332-343. https://doi.org/10.1016/j.cej.2015.12.010

*Corresponding author; email: saowapa.c@psu.ac.th